Energy Conversion and Management 291 (2023) 117255

Contents lists available at ScienceDirect

Energy Conversion and Management

journal homepage: www.elsevier.com/locate/enconman

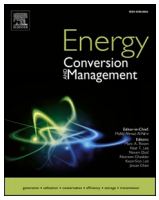

Optimal sizing of a photovoltaic/energy storage/cold ironing system: Life Cycle cost approach and environmental analysis

Daniele Colarossi *, Paolo Principi

Department of Industrial Engineering and Mathematical Sciences, Università Politecnica delle Marche, Via Brecce Bianche 12, Ancona, Italy

ARTICLE INFO

Keywords:
Cold ironing
PV plant
Energy storage
Optimal sizing
Life Cycle Cost
Environmental analysis

ABSTRACT

Traditional cold ironing allows ships to shut down their auxiliary engines, during the berthing time, and to be powered by an on-shore power supply. Traditionally the energy demand is satisfied by electricity form the national grid. Alternatively, a local energy production increases the energetic self-sufficiency of the port areas and reduces the pressure on the national grid with continuous peaks of energy demand. This way the port area can be considered a microgrid, characterized by both energy producers and consumers. This paper presents an optimization model, implemented on MATLAB, to provide the best sizing for a combined photovoltaic/energy storage/cold ironing system. The ferry traffic of the port of Ancona (Italy) has been taken as case study. The proposed model returns the percentage of the energy demand covered, the interactions with the national grid, and the optimal size of the PV plant and the storage capacity basing on a Life Cycle Cost (LCC) approach. Results show that the optimal configurations are 2100 kW and 3600 kW with 5750 kWh (without and with storage system) considering lower initial and operational costs, and 3700 kW and 6400 kW with 17,350 kWh (without and with storage system) hypothesizing higher costs. All scenarios ensure an environmental saving, compared to traditional on-board diesel generators, with 87.4 % maximal CO_2 reduction achieved.

1. Introduction

The maritime traffic of goods and people accounts for around the 2.5 % of the CO_2 global emissions [1], according to the last estimates. In addition, the current trend of traffics is expected to growth in the future, and accordingly the environmental impact of the sector. According to the International Maritime Organization (IMO), the greenhouse gas (GHG) emissions of total shipping sector have increased from 977 million tons in 2012 to 1076 million tons of in 2018, which corresponds to an increase of 9.6 % [2]. The problem is not limited to CO_2, but ships also contribute to NO_x, SO_x and PM emissions in varying degrees depending on the type of engines and fuel used by the ship. It is worth noting mentioning that traditional ships are generally equipped with two different engine types. The main engines are used as ship prime mover, while the auxiliary ones are used to provide uninterrupted power to run the electrical devices and appliances of various systems on board the ship, the so-called hoteling activities. They are intended to supply the essential loads, such as air conditioning, the lighting, the fans, communication devices, alarm systems, and crew living space. During the berthing time of a ship in port, the main engines are turned off, while the auxiliary ones keep running to satisfy the cited services. Usually, auxiliary generators consist of diesel prime mover and alternator [3]and exhaust a considerable amount of air pollutants into the atmosphere [4]. The phenomenon can turn out to be more important especially when ports are located close to the urban areas [5]. Lastly, people living nearby the port also suffer from the continuous noise which is a consequence of the activities carried out simultaneously in a port including those related to berthed ship. For all these reasons, the decarbonization of maritime traffics is a mandatory step to reduce the environmental impact of the sector [6].

Different solutions have been studied and proposed over the years to deal with this problem [7]. Among them, the cold ironing consists in turning off the on-board auxiliary engines of the ship during the berthing time and providing an onshore power supply [89]. So locally, cold ironing ensures a high level of local pollutants abatement allowing a reduction of the environmental impact [10]. Globally, the environmental saving depends on the quality of the energy purchased from the electricity grid [11]. In fact, the higher the quality of the grid energy mix is, the higher the abatement efficiency will be. In case of similar CO_2 emissions, comparing the grid and the on-board engines, the result is a shift of the polluting source from the port to the place where the energy

* Corresponding author.
E-mail address: d.colarossi@pm.univpm.it (D. Colarossi).

https://doi.org/10.1016/j.enconman.2023.117255
Received 6 February 2023; Received in revised form 4 May 2023; Accepted 2 June 2023
Available online 9 June 2023

Nomenclature

a	Discount rate
α_P	PV coefficient of power
BC	Black carbon
C_m	Maintenance cost
C_o	Operation cost
CO_2	Carbon dioxide
DE	Energy deficit
ε	Emission
EF	Emission factor
EP	Engine power
E_{PV}	Demand covered by the PV plant
E_{sold}	Energy given to grid
E_{with}	Energy taken from the grid
E_{sto}	Demand covered by the storage system
f_{pv}	PV derating factor
G_t	Incident radiation
GHG	Greenhouse gas
IMO	International Maritime Organization
LCC	Life Cycle Cost
LNG	Liquefied natural gas
NOCT	Operative PV cell temperature
NO_x	Nitric Oxide
P_i	Power demand by ships
P_v	Energy production
PV	Photovoltaic
q_i	Discount factor
RC	Residual charge
SoC	State of charge
SOx	Sulfur Oxide
STC	Standard test conditions
SU	Energy surplus
t	Berthing time
T_a	Air temperature
T_c	PV cell temperature

is produced [12]. This is relevant to highlight that a clear energy source is mandatory. Several studies have been published aiming to investigate the benefits of an on shore power supply system [13]. Zis [11] proposed a methodology to evaluate the environmental saving obtained by a cold ironing system. The evaluation is based on a comparison between the emission factors of the ships under study and of the electricity grid. Innes and Monios [9] reported the case of the port of Aberdeen, in which the annual savings of CO_2 emissions in port area is about 4767 tons. Herrero et al. [14] investigated the integration of a cold ironing system in the port of Santander. Results show that the emissions reduction is around 37 %. Stolz et al. [15] numerically applied this solution to 714 major ports in the European Economic Area (EEA) and the United Kingdom (UK). Results show that a reduction of 3 Mt CO_2 emissions can be achieved. Hall [16] estimated that the emission savings reaches around 29 % on average, depending on the type of ship and on the call frequency in port, with a peak of 99.5% (Norway) and 85% (France), while only 9.4 % for the Fort Lauderdale port (US), due to the high correlation with the energy mix.

In addition, despite its contribution in reducing the amount of emissions in port [17], the traditional cold ironing, namely powered by the electricity grid, can put pressure on the main electricity grid [18]. In fact, a cold ironing system requires a huge amount of energy from the shore side, especially with the contemporaneity of several ships in port [19]. Generally, ferries can have an energy demand between 1 MW and 3 MW, cruises up to 10 MW and container ships up to 1 MW [20]. Accordingly, a local energy production is required as peak shaving for the main grid, and to increase as much as possible the energetic self-sufficiency of the port [21].

The current trend of local and smart grid must be considered [22]. Traditional grid is designed to transmit electricity from centralized producers to consumers, while in the future multidirectional network the consumers are the producers themselves [23]. This new model can be intended as an energy community, in which the energy produced is shared among members. The local production provides technical benefits [24], such as the reduction of distribution losses and grid congestions [25]. In this sense the integration of renewable sources in local grids is fundamental to produce clean energy, given its proximity to urban areas, and to match the energy demand of ports [26]. In literature different solutions have been proposed and analyzed to simulate local energy production in port areas. Among them, Fioriti et al. [27] investigated an integrated configuration that exploits the LNG cold exergy for the electricity production in port areas. LNG systems have been also investigated and proposed by Borelli et al. [28]. Results showed that the proposed solution ensures a primary energy savings up to 22% compared to traditional technologies. In another work the comparison between shore side and on-board LNG supply has been investigated [29]. The results show that a higher environmental saving have been obtained by using port mitigation than on-board vessels. A cold ironing system powered by a cogeneration plant can provide a good amount of energy to satisfy the energy demand of berthed ships, with a good grade of environmental saving [30]. The increasingly focus on the environmental aspects requires to switch from fossil fuels to renewable energies, such as solar and wind. In this sense, Bakar et al. [26] proposed a microgrid based on renewable energy in supporting the cold ironing. The proposed system includes both photovoltaic system and wind turbines. Kermani et al. [31] also introduced the possibility of energy storage systems to mitigate the intermittent nature of renewable sources. Another solution is the integration of hydrogen-based system in port areas [32].

In this contest, the contribution of this paper is a numerical optimization model aiming to return the best sizing of a photovoltaic plant and the capacity of an energy storage system located in port area. The proposed combined plant is intended to power the cold ironing system by means of the local production of electricity. The proposed model has been developed and implemented on MATLAB and is based on an hourly time step over a one-year period. The chosen parameter for the optimization is the Life Cycle Cost (LCC), as it allows to consider the entire life of the components [33]. The proposed model first provides the match between the energy production and the energy demand, returning the percentage of the energy demand covered and the interactions with the national grid. Then the optimal model returns the optimal size of the PV plant and the energy storage system. The optimization is based on the minimum Life Cycle Cost (LCC). All scenarios proposed have also been investigated as regard the environmental savings. The case of the ferry ships of the port of Ancona (Italy) has been taken as a case study. The periodic presence, during the year, of ferries berthed at the port of Ancona port, which connect the Italian city and the opposite shore of the Adriatic Sea (ports of Croatia, Greece, Montenegro, Albania) and its electricity supply has been taken as a case study.

2. Materials and methods

The optimization model proposed aims to provide the best power plant size to support a cold ironing system. The model is based on a LCC (Life Cycle Cost) approach. The port of Ancona (Italy) has been taken as case study.

The methodology proposed consists in different steps:

Table 1
Energy demand of ships and dwell time at the quay for the case of Ancona (Italy).

	N° generators	EP nominal power (kW)	Summer			Winter		
			N° gen used	Avg. power (kW)	t (h)	N° gen used	Avg. Power (kW)	t (h)
Ship 1	3	2100	1	1600	513.8	1	1600	893.2
Ship 2	3	1400	2	1400 150	314.2	1	1000	845.7
Ship 3	3	1400	2	1400 150	310.8	1	1000	859.5
Ship 4	3	1900	2	1900 300	254.7	2	1900 300	441.2
Ship 5	3	3800	1	2200	310.2	1	2200	433.8
Ship 6	4	850	2	850 350	573.0	2	850 350	253.2
Ship 7	3	1360	1	800	857.3	1	800	1007.8
Ship 8	2	960	1	500	272.2	1	350	131.4
Ship 9	4	783	1	600	871.0	1	600	946.1
Ship 10	3	945	1	800	694.5	1	800	0.0

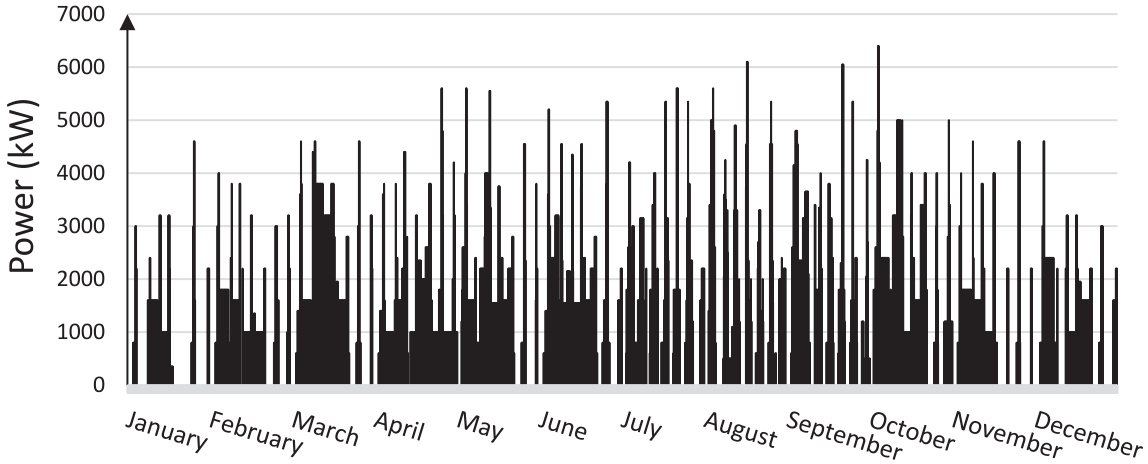

Fig. 1. Annual profile of the energy demand by berthed ships for the case of Ancona (Italy).

- Choice of the type of ships (ferries, cruises, containers etc.).
- Collection of ships characteristics (the nominal and the used power at berth, the duration of the stay and the number of calls).
- Reconstruction of the associated energy demand (a typical week for each month).
- Calculation of the energy production (based on the climatic conditions of the area).
- Simulations and calculation of indexes (energy match, energy interactions with the grid, optimal sizes and environmental saving).

2.1. Choice of the ship types

In this work the analysis is limited to ferry ships, but the methodology remains valid for all kind of ships. Ferries are characterized by a regular frequency of calls in port, and a medium energy demand compared to cruises (higher power required) and container ships (lower power required). The calculation of the overall energy demand for the port is hourly based over a period of one year. Table 1 summarizes the ferry ships considered in this work. Each ship is equipped with a different number of auxiliary generators, in this case ranging from two to four. The nominal power indicates the maximum power of each generator, while the actual value has been considered basing on the usual average energy demand of the ships. Data are differentiated between summer and winter season, as a different power is required by ships for the internal activities (air conditioning, lighting etc.).

2.2. Energy demand

The energy demand profile (Fig. 1) has been reconstructed considering the typical week of each month. The energy demand is related to the contemporaneity of ships in port. The power required by the ships at a certain time i (hour), Pi, can be calculated with the following equation (Eq. (1) [21]:

$$P_i = P_{i-1} + P_a - P_d \qquad \text{(kW)} \tag{1}$$

where P_{i-1} is the power required by ships at berth at the previous time step, Pa is the power of the ships that arrives in the port at time i, and Pd is the power demand of the ships that departs from the port. Eq. (1) has been solved for the year under analysis (considering the reference traffic of the port of Ancona) and the final trend is reported in Fig. 1. The energy demand turns out to be very variable during the different weeks and seasons and ranges between 0 W, in absence of ships in port, to 6400 kW, during the maximum contemporaneity of ships in port.

2.3. Energy production

As regard the energy production, the first proposed scenarios consist of a simple PV system, located in port area, that provides energy to meet the demand for electricity of berthed ships. In absence of solar radiation or when the energy demand is higher that the produced one, the electricity is taken from the national grid. In case of energy surplus, which means that the energy production is higher than the energy demand of

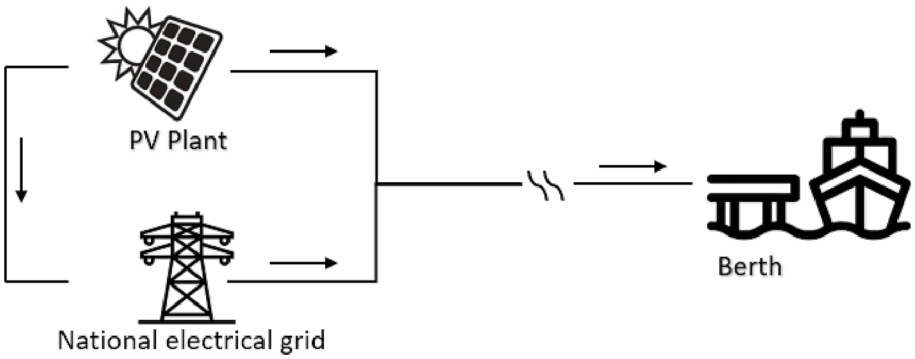

Fig. 2. Plant scheme of the simple photovoltaic scenario (arrows indicate the energy flows).

ships, the energy is given to the national grid. The data required for the calculation of the production by a PV system are the ambient temperature and the irradiance. Data of the weather conditions of Ancona (Italy) were collected from 01/08/2018 to 31/07/2019, on an hourly basis. The output power (P_{PV}) is calculated with the following equation (Eq. (2) [34 35]:

$$P_{PV} = P_r \bullet f_{PV} \bullet \left(\frac{G_T}{G_{T,STC}}\right) \bullet \left[1 + \alpha_p \bullet \left(T_C - T_{C,STC}\right)\right] \ (kW) \quad (2)$$

where P_r is the rated capacity of the PV array, meaning its power output under standard test conditions (kW). f_{PV} is the PV derating factor (%), G_T the solar radiation incident on the PV array in the current time step (W/m^2), $G_{T,STC}$ the incident radiation at standard test conditions. α_P is the temperature coefficient of power (%/°C), TC the PV cell temperature in the current time step (°C) and $T_{C,STC}$ the PV cell temperature under standard test conditions. STC (Standard Test Conditions) refers to 1000 W/m^2 of solar radiation and 25 °C of air temperature. In fact, the cell temperature during the working time of a PV panel can be expressed as a function of the ambient temperature and the incident solar radiation on the panel (Eq. (3):

$$T_C = T_a \bullet G_t \bullet \left(\frac{NOCT - 20}{800}\right) \quad (°C) \quad (3)$$

where Ta is the ambient temperature at the current time step (°C) and the NOCT is the operative temperature of the PV panel. In this study, considering monocrystalline PV panels, the NOCT is assumed to be 45 °C [34] and the coefficient of power α_P is equal to – 0.5 %/°C [36]. The PV derating factor f_{PV} is equal to 93 % [37].

2.4. Economic analysis

The economic analysis proposed is based on a Life Cycle Cost approach (LCC). This method has been chosen as it allows to consider both the initial investment costs and the operation and maintenance costs throughout the life of the system (life cycle), and eventually the residual value at the end of the life cycle (disposal phase). The method provides a good overview of the configuration as it involves both the energetic and economic aspect. The LCC index can be calculated as follow (Eq. (4):

$$LCC_i = C_I + \sum_{t=1}^{n} \frac{C_{M,i} + C_{O,i}}{q^i} \quad (€) \quad (4)$$

and the objective function is the one that minimize the LCC (Eq. (5),

$$LCC_{min} = \min f(LCC) \quad (€) \quad (5)$$

where C_I is the initial investment costs, $C_{M,i}$ and $C_{O,i}$ are the maintenance and operation costs over the period i, respectively. The parameter q_i is defined as $(a + 1)^i$, where "a" is the discount rate during the n- years of the project (life cycle). Investment costs involve the purchase of the plant and the connection from shoreside to shipside, while annual costs include energy costs for the energy taken from the grid and the maintenance. The LCC method allows to compare different scenarios, by varying both the PV plant size and the energy storage capacity. The best scenario is the one with the lowest LCC index.

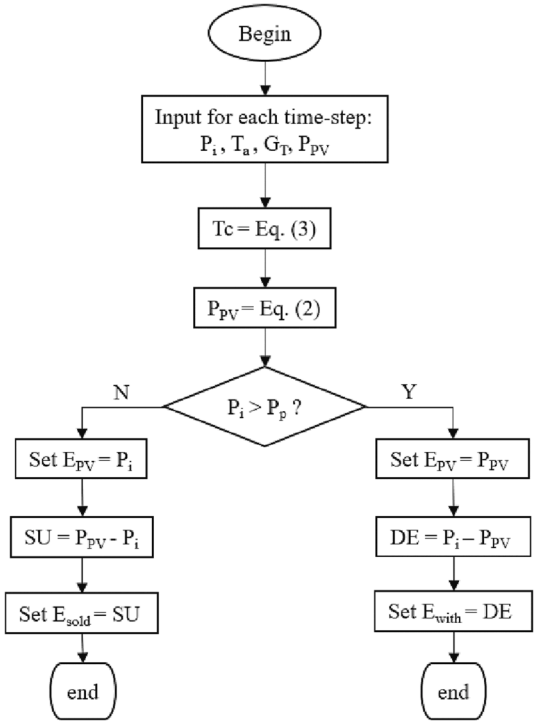

Fig. 3. Flow chart of the photovoltaic scenario.

2.5. Optimization models

Different numerical models have been developed and implemented on MATLAB, depending on the presence of the storage system. At first the simpler numerical model is presented, namely the PV plant/cold ironing. Then the energy storage system is added to the model. Both models are based on a LCC approach for the optimization.

2.5.1. Simple PV/cold ironing

In the simpler scenario, only the photovoltaic plant is present. This means that only a direct match between energy demand (ships) and energy production (PV plant) is allowed. Fig. 2 summarizes the plant scheme of the first proposed configuration.

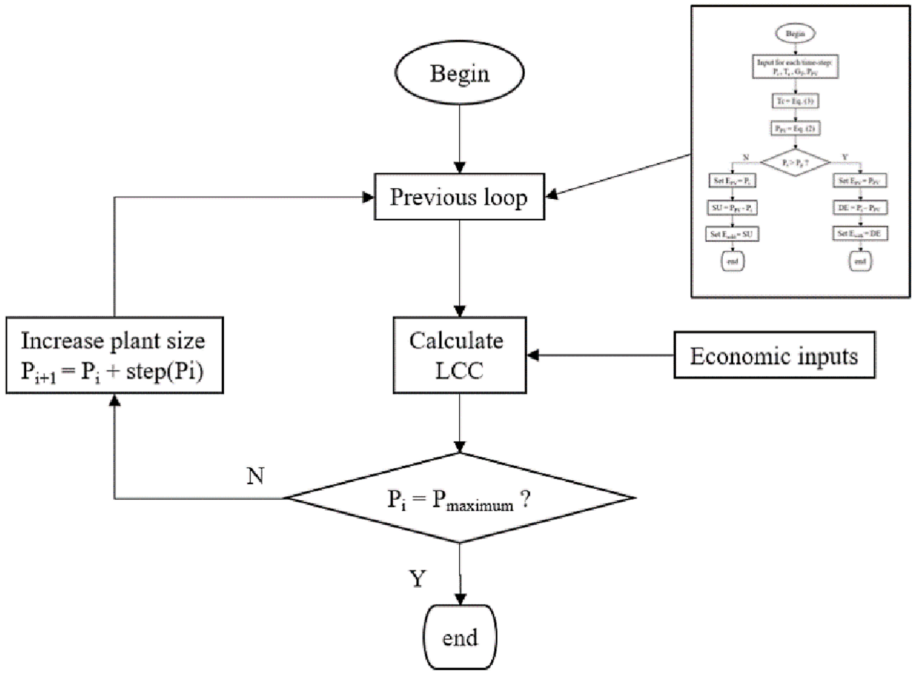

Fig. 4. Flow chart of LCC loop of the simple PV/cold ironing plant.

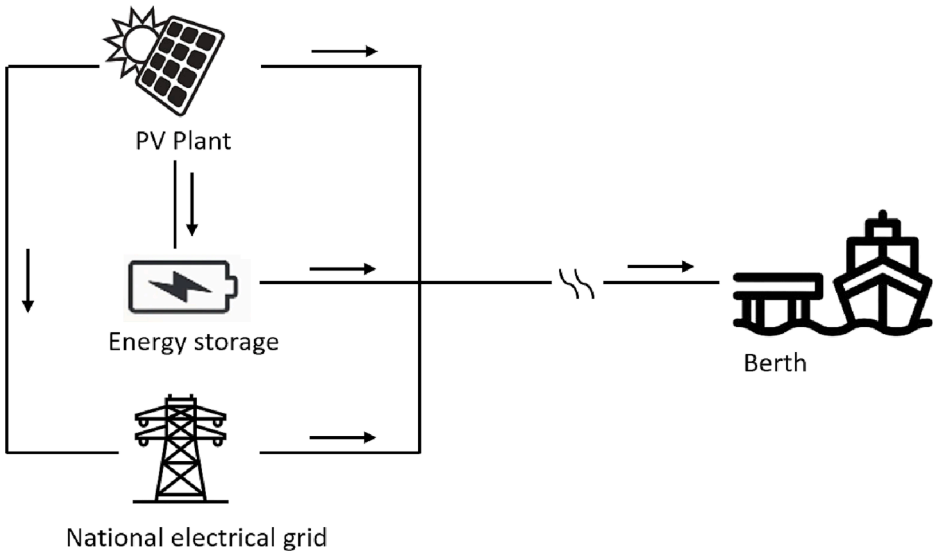

Fig. 5. Plant scheme of the photovoltaic/energy storage scenario (arrows indicate the energy flows).

The first model determines the share of the energy demand of ships at berth directly covered by the photovoltaic plant. The remaining share is taken from the grid. The input data are the solar radiation (G_T), the ambient temperature (T_a), the power required by ships (P_i) and the PV plant size (P_{pv}). The model consists in a comparison, for each time step (hourly), between energy demand and production. The model calculates and returns the PV production according to Eq. (2) and Eq. (3), and then matches, for each time step over one year, the energy production and the energy demand. At each time step, in presence of ships in port, allocates the share of energy to the PV plant or to the grid. In absence of ships, the eventual energy production is directly given to the grid. The diagram flow of the model is depicted in Fig. 3, where E_{pv} is the energy provided by the PV plant to ships, SU is the energy surplus and DE is the energy deficit.

The single scenario (single P_{pv} value) is involved in the optimization tool based on the minimization of the LCC index. as shown in Eq. (4). The optimization loop consists in solving the previous model, calculating the LCC and then increasing the PV plant size at each step, repeating the loop up to designed maximal value (Fig. 4). The input data are the results of the previous model, namely the share of the energy demand provided by the PV plant and by the grid, and in addition the economic, namely initial, operation and maintenance costs. The model returns the LCC index, considering a life cycle of 20 years of the plant [38]. Then the loop is repeated by increasing the PV plant size of a power step. For each scenario the LCC index is calculated and at the end the optimal size of the plant is highlighted (the one with the lowest LCC). Fig. 4 shows the flow chart. In addition for each step the interactions with the grid is highlighted, both the energy taken and given to the grid. This can be a useful parameter to investigate the self-sufficiency of the scenario and the weight on the grid.

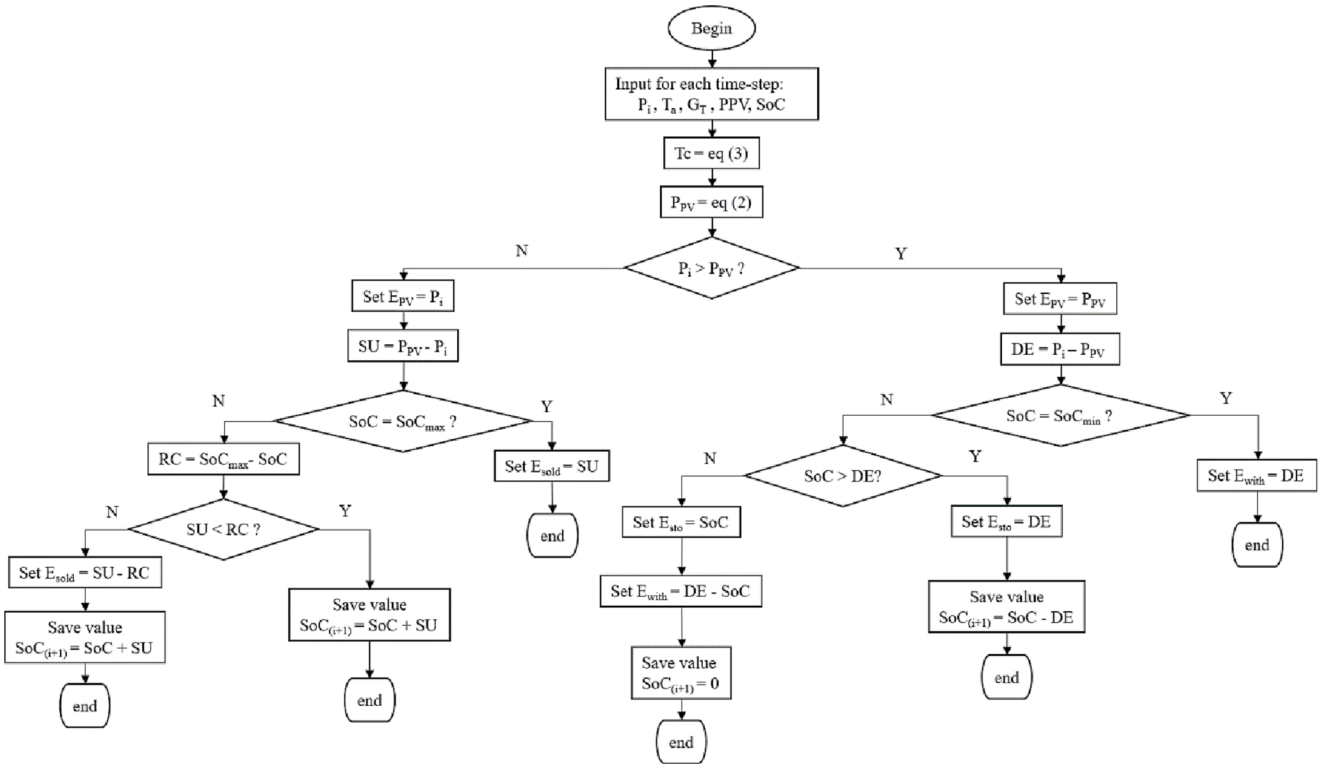

Fig. 6. Flow chart of a photovoltaic/energy storage scenario.

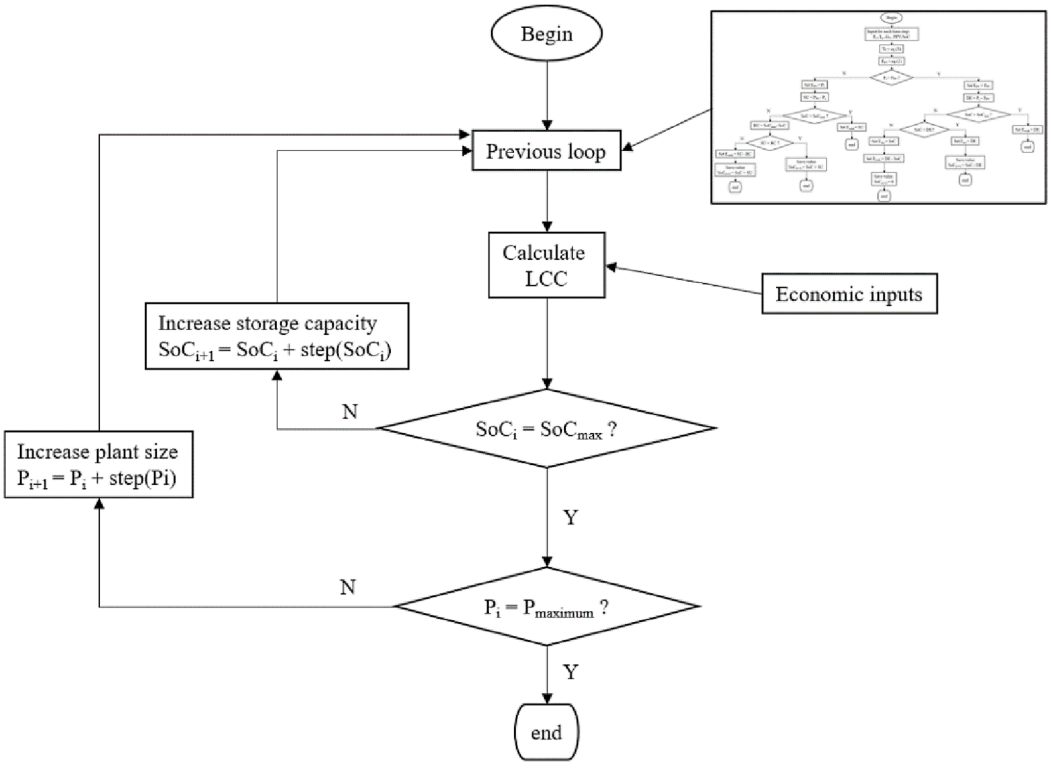

Fig. 7. Diagram flow of LCC loop of the PV/energy storage/cold ironing scenario.

2.5.2. PV/energy storage/cold ironing

The model consists in two parts, as for the simple PV case. The first model allocates the share of energy to the PV plant, to the storage system and to the grid, while the second one, the LCC loop, provides the optimization tool and determines the best PV plant and storage system sizes. Fig. 5 summarizes the plant scheme of the first proposed configuration.

In addition to the simpler case, in this model the storage capacity is

Table 2
Emission factors (kg/kWh) for grid and (kg/ kg of fuel) for ships.

	CO_2	SO_2	NO_x	BC
Ships	3.082	0.022	0.057	3.37E-03
Grid	0.258	4.81E-05	2.11E-04	3.99E-08

also defined, expressed as State of Charge (SoC). The first step is the energy production calculation (Eq. (2) and Eq. (3). Then, as for the previous model, the energy demand and production are compared. In this case, when the energy demand is more than the energy production (energy deficit), the model checks the state of charge, residual charge (RC) in the diagram flow, of the storage system and if possible, allocates the energy demand to the latter (E_{sto}). On the contrary, when the energy demand is less than the energy production (energy surplus), the model checks the state of charge before giving the surplus to the grid. In case, the storage system can be charged up to the maximum state of charge. The steps are depicted in the flow chart of Fig. 6.

Once the single scenario is solved, the optimization loop optimizes the sizes, both the PV plant and the storage capacity (Fig. 7). The model consists in a scan of a matrix, which has for rows and columns the steps of PV plant size and storage capacity. The two properties can be expressed as follow:

$PV = \{PV_0, PV_1, \ldots, PV_i, \ldots, PV_n\}$.

$SoC_{max} = \{SoC_{max,0}, SoC_{max,1}, \ldots, SoC_{max,i}, \ldots, SoC_{max,n}\}$.

For each pair the LCC is calculated. At the beginning, the first PV plant size is set, and all the storage capacities are simulated by increasing in each cycle. Then the loop is repeated for the second PV plant size and so on up the maximum PV plant size (PV_n). Results can be visualized as 3D curve, where the z-axis is the LCC. This way the best scenario can be selected.

2.6. Environmental analysis

The environmental analysis aims, once the best scenario has been determined, to provide the emission saving. The method compares the pollutant emissions of the auxiliary engines of ships, usually diesel generators, with the emission factor of the energy mix of the grid. The analysis is provided for a list of pollutants, namely CO_2, NO_x, SO_x and BC, which can be considered the most common. The environmental emission of a pollutant is calculated with the following equations (Eq. (6)):

$$\varepsilon_i = EF_i \bullet E_i \quad \text{(kg)} \tag{6}$$

where ε_i (kg) is the amount of emission of the pollutant "i", EF_i is the emission factor and E_i (kWh) is the energy withdrawn from the electrical grid. The emission factors are expressed as "kg/kWh" for the energy taken from the grid and as "kg/kg of fuel" for the traditional fuel used by the ships. Results will strongly depend on the quality of the energy mix considered. The more the energy mix is qualitative (with a large share of renewable energy), the more the saving obtained will be. In this study, the values of the emission factors are taken from the Italian energy mix (from the inventory of SINAnet ISPRA [39]). The emission factors are summarized in Table 2.

3. Results and discussions

3.1. Simple PV/cold ironing

In addition to the traditional cold ironing, two different scenarios have been simulated, characterized by different initial and operation costs:

- Traditional cold ironing, namely the energy demand is fully satisfied by the national grid.
- "Scenario 1", where the PV plant size is optimized with 1400 €/kW [40] as initial cost of the PV plant and 0.2 €/kWh [41] as energy cost for the share withdrawn from the national grid.
- "Scenario 2", where the PV plant size is optimized with 1800 €/kW as initial cost of the PV plant and 0.4 €/kWh as energy cost for the share withdrawn from the national grid. This scenario hypothesizes a spike of energy and material prices.

The first result analyzed is the direct match between the energy production (PV plant) and the energy demand (berthed ships). Both trends are characterized by a high grade of variability. In fact, the energy demand on the presence of ships in port, while the PV production strongly depends on the presence of the solar radiation. The simulation has been launched for a range of PV plant size from 1000 kW to 10000 kW, with a power step of 100 kW. The resulting match is shown in Fig. 8.

The match increases with the PV plant size, as expected. The share ranges from 9.5% (for the 1000 kW PV plant) to 42 % (for the 10000 kW PV plant case). The curve is not linear, in fact while the PV plant size increases, the slope tends to become horizontal. The reason is that a

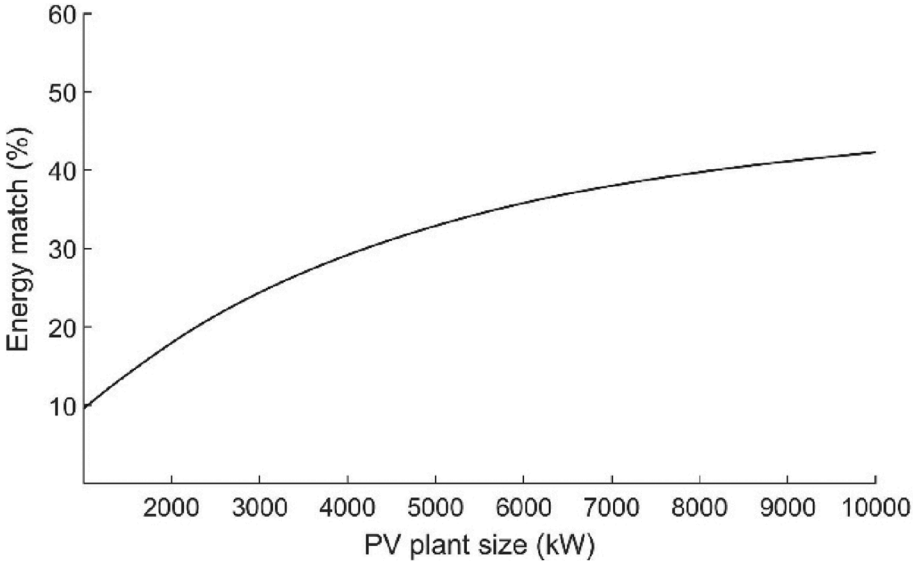

Fig. 8. Energy match (%) between energy production and demand.

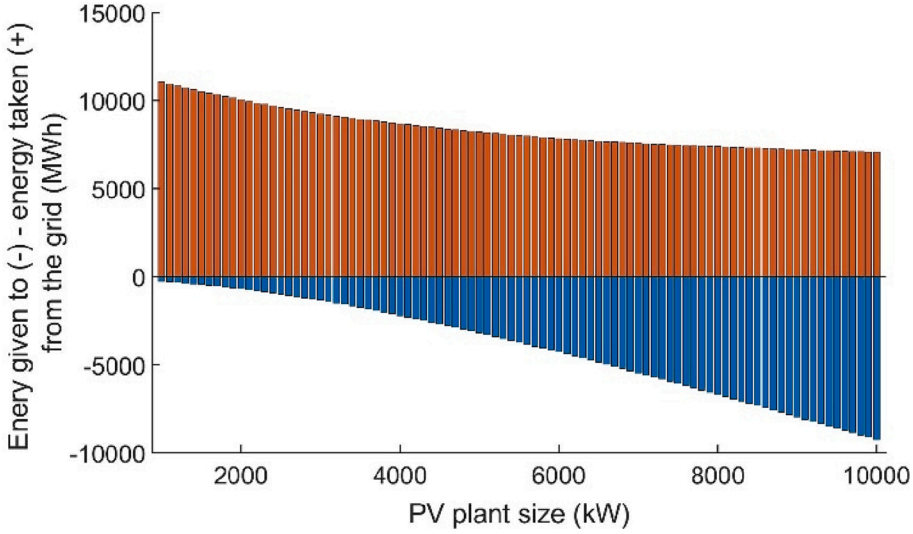

Fig. 9. Energy interaction with the grid.

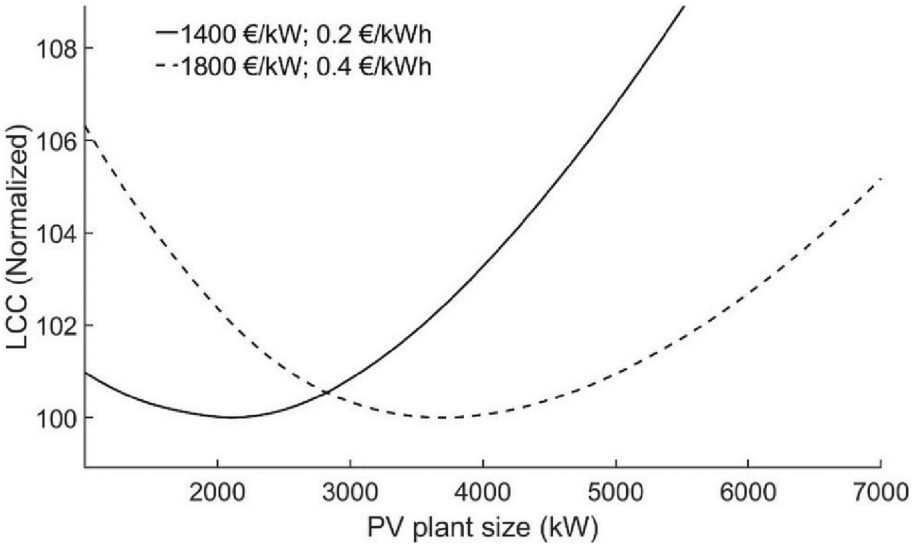

Fig. 10. LCC optimization for the two scenarios considered.

share of the energy demand occurs in period of absence of energy production (such as at night) and accordingly is independent from the size of the plant. In addition, as shown in Fig. 9, increasing the size of the PV plant, there is an increase of the energy surplus, which is given to the national grid. The figure shows the energy interactions with the grid, where the red bars (above zero) indicate the energy deficit withdrawn from the grid, while the blue bars (below zero) indicate the energy surplus given to the grid. This phenomenon has been investigated for the same range of PV plant power plants, from 1000 kW to 10000 kW. Result is shown in Fig. 9.

It is clearly visible that increase the PV plant size produces an increase of the energy surplus given to the grid, while the energy taken from the grid remains almost constant (after a first zone of reduction). This is due to the mismatch between energy demand and production, which is not covered by increasing the PV plant size.

The optimization model returns the best PV plant size LCC-based. The model presented has been simulated for both scenarios. The best PV plant size turns out to be 2100 kW (with a LCC of 23.1 M€) for the scenario with average prices (scenario 1), while 3700 kW (with a LCC of 42.7 M€) for the one considering a spike of prices (scenario 2). In Fig. 10 the values of LCC have been normalized to better compare the two scenarios, setting a reference value of 100 to the minimum LCC.

$$\mathrm{LCC}_{norm} = \frac{LCC_i}{LCC_{min}} \bullet 100 \tag{7}$$

3.2. PV/energy storage/cold ironing system

As regard the storage-integrated system, two different scenarios have been simulated, called “scenario 3” and “scenario 4”, characterized by different costs:

- “Scenario 3”, where the initial cost of the PV plant and of the storage system are 1400 €/kW and 200 €/kWh, respectively, and 0.2 €/kWh is the energy cost for the share of energy demand withdrawn from the national grid.
- “Scenario 4”, where the initial cost of the PV plant and of the storage system are 1800 €/kW and 250 €/kWh [42], respectively, and 0.4 €/kWh is the energy cost for the share of energy demand withdrawn from the national grid. This scenario hypothesizes a spike of energy and material prices.

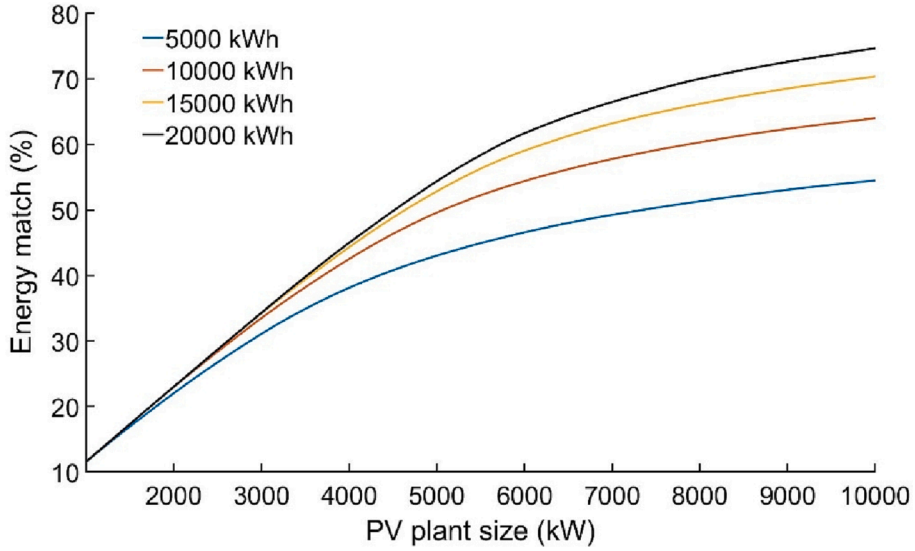

Fig. 11. Energy match (%) between energy production and demand (energy storage included).

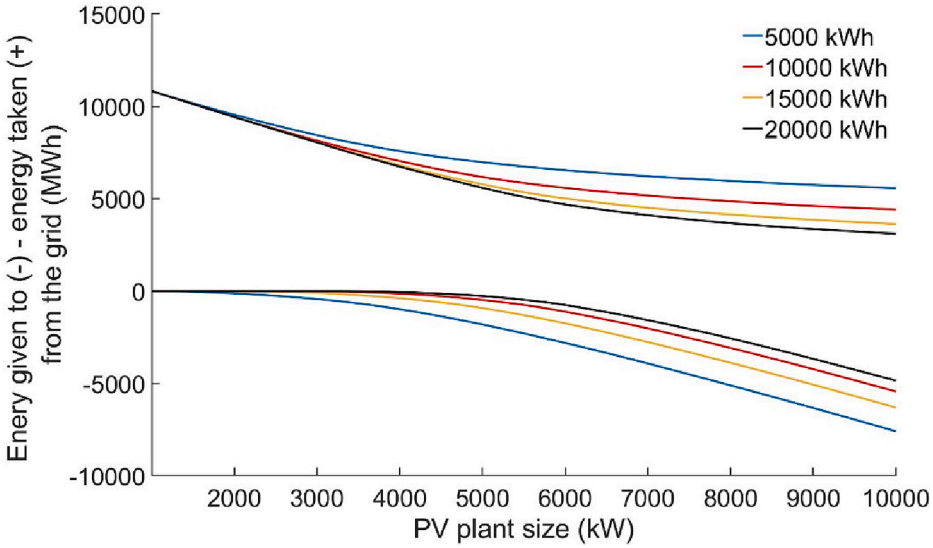

Fig. 12. Energy interaction with the grid (energy storage included).

It's worth mentioning that the battery life (10 years [43]) is lower than the life cycle considered for the whole system. Accordingly in the calculation of the costs the replacement of the energy storage system is involved. In the simulations, the PV plant size ranges from 1000 kW to 10000 kW, with a power step of 100 kW, while the values of the energy storage capacity range from 1000 kWh to 20,000 kWh, with a capacity step of 100 kWh. For a matter of more clarity, the energy match between the energy production (PV plant) and the energy demand (berthed ships) has been plotted for four different energy storage system sizes (from 5000 kWh to 20,000 kWh, with a step of 5000 kWh). Results are shown in Fig. 11.

It is clearly visible that the energy match between the energy production and the energy demand increases both with the PV plant size and with the storage capacity. In addition, the contribution of the storage system increases with the PV power. In fact, at low PV plant sizes the storage system does not increase the percentage of energy match, due to the lower amount of energy surplus to be stored. For a PV plant size of 10000 kW, the energy match ranges between 54.5 % (for a storage capacity of 5000 kWh) and 74.6 % (for a storage capacity of 20,000 kWh), compared to the 42 % for the simple PV plant case. The relation between energy match and storage capacity, at a given PV plant size, is not linear, but decreases while increasing the storage capacity. In fact, the energy match turns out to be 54.5 %, 64 %, 70.3 % and 74.6 % for a storage capacity of 5000 kWh, 10,000 kWh, 15,000 kWh and 20,000 kWh, respectively. The marginal increase, for steps of 5000 kWh, is 9.5 %, 6.3 % and 4.3 %, respectively.

The increasing of the self-sufficiency of the proposed system allows the energy interactions with the grid to be reduced. This way, the pressure of the energy demand on the local/national grid is lower. As for the simpler case, the energy taken from the grid decreases while increasing the PV plant size. Vice versa for the energy given to the grid, which increase with the PV plant size, as shown in Fig. 12. The contribution of different storage capacity sizes increases with the PV plant size. Numerically at 10000 kW, the energy taken from the grid is 5569 MWh (5000 kWh), 4408 MWh (10000 kWh), 3627 MWh (15000 kWh) and 3100 MWh (20000 kWh). These values correspond to a reduction of 22.2 % (5000 kWh), 38.7 % (10000 kWh), 48.7 % (15000 kWh) and 56.2 % (20000 kWh), compared to the 7066 MWh of the simple PV plant scenario. As regard the energy given to the grid, the reductions are 18 % (5000 kWh), 31.9 % (10000 kWh), 41.3 % (15000 kWh) and 47.6 %

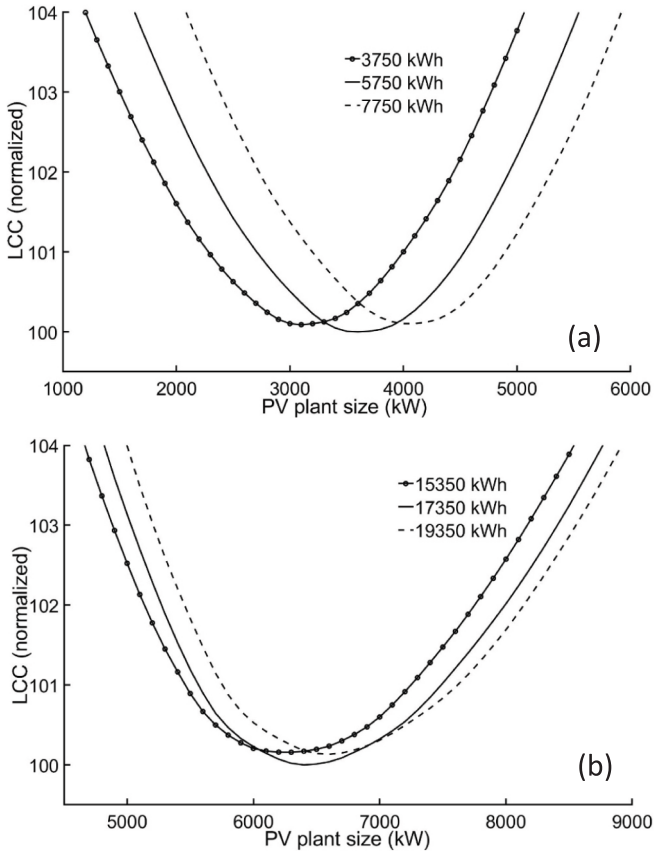

Fig. 13. Energy interaction with the grid for scenario 3 (a) and scenario 4 (b).

(20000 kWh), compared to the 9260 MWh of the simple PV plant scenario.

The optimization tool is fundamental to determine the best configuration for the proposed system. As for the simpler case, two different scenarios have been simulated, to show the flexibility of the proposed model. Fig. 13a shows the results for scenario 3, the one with initial and operational costs on the averages. The best sizes for the PV plant and the energy storage system turn out to be 3600 kW and 5750 kWh, respectively. The LCC value is 22.5 M€. In Fig. 13, the normalized LCC (with the lowest value equal to 100) has been represented for an easier visualization. By comparing scenario 1 and 3, both with the lower prices, the addition of the energy storage system allows to increase the PV plant size (from 2100 kW to 3600 kW). Fig. 13b shows the results for scenario 4, with prices above the averages. In this case the best sizes for the PV plant and the energy storage system turn out to be 6400 kW and 17,350 kWh, respectively. Higher prices justify larger PV plant and storage system sizes. The LCC values is 36.7 M€.

The environmental analysis has been performed only for the best configuration of each scenario. For each of them the environmental saving has been compared to the conventional scenario, namely the pollutants emitted by the on-board diesel generators of berthed ships. Fig. 12 summarizes the environmental savings obtained for the pollutants studied (CO_2, NO_X, SO_X, BC). The first bars on the left ("Ref. case") refers to the traditional cold ironing, entirely powered by the national grid. As expected, the percentage of saving increases with the self-sufficiency resulting of the scenario, both by increasing the PV plant size and the storage capacity. Results for the all the pollutants considered are summarized in Fig. 14 It is worth noting that the percentages of saving obtained depends on the energy mix considered. In this case, the Italian energy mix has been considered.

4. Conclusions

This work deals with the environmental pollution caused by ships in port, during their berthing time. A cold ironing system replaces the on-board diesel generators with an onshore power supply powered by the electricity grid, and this way allows to reduce the environmental impact. This paper presents an optimization model for a combined photovoltaic/energy storage/cold ironing system. The ferries traffic of the port of Ancona (Italy) has been taken as case study. A numerical model has been implemented on MATLAB. The model investigates the match between the energy demand (auxiliary engines of berthed ships) and the energy production (photovoltaic plant in port area), with and without an energy storage system. Results, regarding the energy match between production and demand, show that:

- The percentage of energy match ranges between 9.5 % (for a PV plant of 1000 kW) to 42 % (for the 10000 kW case) without energy storage.
- The same percentages range between 10.9 % and 74.6 % increasing the energy storage capacity up to 20,000 kWh.
- The energy given to the national grid increases with the PV plant size, while the energy taken from the grid remains almost constant at high PV plant size.

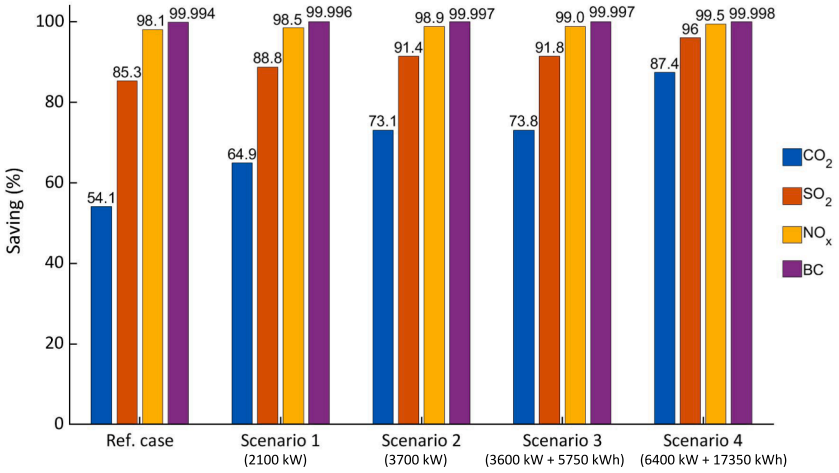

Fig. 14. Saving of polluting emissions.

- Considering the configuration with the maximum storage capacity, the energy taken from the grid is reduced by 22.2 %. As regard the energy given to the grid, the reduction is 47.6 %, compared to the simple PV plant scenario.

The optimization of the PV plant size and the storage capacity have been performed basing on a Life Cycle Cost (LCC) approach. Results show that:

- The optimal plant size is 2100 kW for the scenario with average prices, while 3700 kW considering a spike of prices, both without considering an energy storage system.
- With the energy storage system, the optimal sizes are 2100 kW and 3600 kW with 5750 kWh (without and with storage system) considering lower initial and operational costs, and 3700 kW and 6400 kW with 17,350 kWh (without and with storage system) hypothesizing higher costs.
- The environmental analysis shows that a traditional cold ironing (energy demand fully provided by the national grid) allows a reduction of the CO_2 emissions of 54.1 %. The two scenarios resulting from the optimization model ensure a CO_2 emission saving equal to 64.9 % and 73.1 %, respectively.

The present paper proves that a local energy production, from renewable sources, can provide a good self-sufficiency in supplying the energy demand of berthed ships. This reduces the pressure on the electricity grid, as it smooths the continuous peak of energy demand. The proposed model can be extended by adding the energy production by wind turbines in parallel to solar energy.

CRediT authorship contribution statement

Daniele Colarossi: Conceptualization, Methodology, Validation, Investigation, Resources, Visualization, Supervision. **Paolo Principi:** Conceptualization, Methodology, Validation, Investigation, Resources, Visualization, Supervision.

Declaration of Competing Interest

The authors declare that they have no known competing financial interests or personal relationships that could have appeared to influence the work reported in this paper.

Data availability

Data will be made available on request.

References

[1] Yuan J, Nian V. Ship energy consumption prediction with Gaussian process metamodel. Energy Procedia 2018;152:655–60. https://doi.org/10.1016/j.egypro.2018.09.226.

[2] I. International Maritime Organization, Highlights and Executive Summary of the Fourth IMO GHG Study 2020 HIGH, (n.d.).

[3] Lou H, Hao Y, Zhang W, Su P, Zhang F, Chen Y, et al. Emission of intermediate volatility organic compounds from a ship main engine burning heavy fuel oil. J Environ Sci (China) 2019;84:197–204. https://doi.org/10.1016/j.jes.2019.04.029.

[4] Huang L, Wen Y, Geng X, Zhou C, Xiao C. Integrating multi-source maritime information to estimate ship exhaust emissions under wind, wave and current conditions. Transp Res Part D Transp Environ 2018;59:148–59. https://doi.org/10.1016/j.trd.2017.12.012.

[5] Dragović B, Tzannatos E, Tselentis V, Meštrović R, Škurić M. Ship emissions and their externalities in cruise ports. Transp Res Part D Transp Environ 2018;61:289–300. https://doi.org/10.1016/j.trd.2015.11.007.

[6] Bakar NNA, Guerrero JM, Vasquez JC, Bazmohammadi N, Yu Y, Abusorrah A, et al. A review of the conceptualization and operational management of seaport microgrids on the shore and seaside. Energies 2021;14:1–31. https://doi.org/10.3390/en14237941.

[7] Tichavska M, Tovar B, Gritsenko D, Johansson L, Jalkanen JP. Air emissions from ships in port: Does regulation make a difference? Transp Policy 2019;75:128–40. https://doi.org/10.1016/j.tranpol.2017.03.003.

[8] Williamsson J, Costa N, Santén V, Rogerson S. Barriers and Drivers to the Implementation of Onshore Power Supply—A Literature Review. Sustainability 2022;14:1–16.

[9] Innes A, Monios J. Identifying the unique challenges of installing cold ironing at small and medium ports – The case of aberdeen. Transp Res Part D Transp Environ 2018;62:298–313. https://doi.org/10.1016/j.trd.2018.02.004.

[10] Iris Ç, Lam JSL. Optimal energy management and operations planning in seaports with smart grid while harnessing renewable energy under uncertainty. Omega (United Kingdom) 2021;103:102445. https://doi.org/10.1016/j.omega.2021.102445.

[11] Zis TPV. Prospects of cold ironing as an emissions reduction option. Transp Res Part A Policy Pract 2019;119:82–95. https://doi.org/10.1016/j.tra.2018.11.003.

[12] Dai L, Hu H, Wang Z. Is Shore Side Electricity greener? An environmental analysis and policy implications. Energy Policy 2020;137:111144. https://doi.org/10.1016/j.enpol.2019.111144.

[13] Nguyen DH, Lin C, Cheruiyot NK, Hsu JY, Cho MY, Hsu SH, et al. Reduction of nox and so2 emissions by shore power adoption, Aerosol Air. Qual Res 2021;21:1–12. https://doi.org/10.4209/aaqr.210100.

[14] Herrero A, Ortega Piris A, Diaz-Ruiz-Navamuel E, Gutierrez MA, Lopez-Diaz AI. Influence of the Implantation of the Onshore Power Supply (OPS) System in Spanish Medium-Sized Ports on the Reduction in CO2 Emissions: The Case of the Port of Santander (Spain). J Mar Sci Eng 2022;10:10101446. https://doi.org/10.3390/jmse10101446.

[15] Stolz B, Held M, Georges G, Boulouchos K. The CO2 reduction potential of shore-side electricity in Europe. Appl Energy 2021;285:116425. https://doi.org/10.1016/j.apenergy.2020.116425.

[16] Hall WJ. Assessment of CO2 and priority pollutant reduction by installation of shoreside power. Resour Conserv Recycl 2010;54:462–7. https://doi.org/10.1016/j.resconrec.2009.10.002.

[17] Spengler T, Tovar B. Potential of cold-ironing for the reduction of externalities from in-port shipping emissions: The state-owned Spanish port system case. J Environ Manage 2021;279:111807. https://doi.org/10.1016/j.jenvman.2020.111807.

[18] Kumar J, Palizban O, Kauhaniemi K. Designing and analysis of innovative solutions for harbour area smart grid, 2017 IEEE Manchester PowerTech. Powertech 2017;2017:7980870. https://doi.org/10.1109/PTC.2017.7980870.

[19] Martínez-López A, Romero-Filgueira A, Chica M. Specific environmental charges to boost Cold Ironing use in the European Short Sea Shipping. Transp Res Part D Transp Environ 2021;94:102775. https://doi.org/10.1016/j.trd.2021.102775.

[20] Iris Ç, Lam JSL. A review of energy efficiency in ports: Operational strategies, technologies and energy management systems. Renew Sustain Energy Rev 2019;112:170–82. https://doi.org/10.1016/j.rser.2019.04.069.

[21] Rolan A, Manteca P, Oktar R, Siano P. Integration of Cold Ironing and Renewable Sources in the Barcelona Smart Port. IEEE Trans Ind Appl 2019;55:7198–206. https://doi.org/10.1109/TIA.2019.2910781.

[22] Vichos E, Sifakis N, Tsoutsos T. Challenges of integrating hydrogen energy storage systems into nearly zero-energy ports. Energy 2022;241:122878. https://doi.org/10.1016/j.energy.2021.122878.

[23] Pérez Osses JR, Palma VM, Reusser CA. Emissions assessment of a tanker in a chilean port using bi-directional cold ironing integrated to LNG. Sustain Energy Technol Assessments 2022;52:102135. https://doi.org/10.1016/j.seta.2022.102135.

[24] Hoang AT, Foley AM, Nižetić S, Huang Z, Ong HC, Ölçer AI, et al. Energy-related approach for reduction of CO2 emissions: A strategic review on the port-to-ship pathway. J Clean Prod 2022;355:131772. https://doi.org/10.1016/j.jclepro.2022.131772.

[25] Sciberras EA, Zahawi B, Atkinson DJ. Electrical characteristics of cold ironing energy supply for berthed ships. Transp Res Part D Transp Environ 2015;39:31–43. https://doi.org/10.1016/j.trd.2015.05.007.

[26] Bakar NNA, Guerrero JM, Vasquez JC, Bazmohammadi N, Othman M, Rasmussen BD, et al. Optimal Configuration and Sizing of Seaport Microgrids including Renewable Energy and Cold Ironing—The Port of Aalborg Case Study. Energies 2022;15:2022. https://doi.org/10.3390/en15020431.

[27] Fioriti D, Baccioli A, Pasini G, Bischi A, Migliarini F, Poli D, et al. LNG regasification and electricity production for port energy communities: Economic profitability and thermodynamic performance. Energy Convers Manag 2021;238:114128. https://doi.org/10.1016/j.enconman.2021.114128.

[28] Borelli D, Devia F, Schenone C, Silenzi F, Tagliafico LA. Dynamic modelling of LNG powered combined energy systems in port areas. Energies 2021;14:14123640. https://doi.org/10.3390/en14123640.

[29] Martínez-López A, Romero A, Orosa JA. Assessment of cold ironing and LNG as mitigation tools of short sea shipping emissions in port: A Spanish case study. Appl Sci 2021;11:1–16. https://doi.org/10.3390/app11052050.

[30] Colarossi D, Principi P. Technical analysis and economic evaluation of a complex shore-to-ship power supply system. Appl Therm Eng 2020;181. https://doi.org/10.1016/j.applthermaleng.2020.115988.

[31] Kermani M, Shirdare E, Parise G, Bongiorno M, Martirano L. A Comprehensive Technoeconomic Solution for Demand Control in Ports: Energy Storage Systems Integration. IEEE Trans Ind Appl 2022;58:1592–601. https://doi.org/10.1109/TIA.2022.3145769.

[32] Sifakis N, Vichos E, Smaragdakis A, Zoulias E, Tsoutsos T. Introducing the cold-ironing technique and a hydrogen-based hybrid renewable energy system into ports. Int J Energy Res 2022;46:20303–23. https://doi.org/10.1002/er.8059.

[33] Colarossi D, Lelow G, Principi P. Local energy production scenarios for emissions reduction of pollutants in small-medium ports. Transp Res Interdiscip Perspect 2022;13. https://doi.org/10.1016/j.trip.2022.100554.
[34] Ceylan İ, Yilmaz S, İnanç Ö, Ergün A, Gürel AE, Acar B, et al. Determination of the heat transfer coefficient of PV panels. Energy 2019;175:978–85. https://doi.org/10.1016/j.energy.2019.03.152.
[35] Tang R, Li X, Lai J. A novel optimal energy-management strategy for a maritime hybrid energy system based on large-scale global optimization. Appl Energy 2018; 228:254–64. https://doi.org/10.1016/j.apenergy.2018.06.092.
[36] Dimri N, Tiwari A, Tiwari GN. Thermal modelling of semitransparent photovoltaic thermal (PVT) with thermoelectric cooler (TEC) collector. Energy Convers Manag 2017;146:68–77. https://doi.org/10.1016/j.enconman.2017.05.017.
[37] Masrur H, Konneh KV, Ahmadi M, Khan KR, Othman ML, Senjyu T. Assessing the techno-economic impact of derating factors on optimally tilted grid-tied photovoltaic systems. Energies 2021;14:14041044. https://doi.org/10.3390/en14041044.
[38] Muhsen DH, Khatib T, Abdulabbas TE. Sizing of a standalone photovoltaic water pumping system using hybrid multi-criteria decision making methods. Sol Energy 2018;159:1003–15. https://doi.org/10.1016/j.solener.2017.11.044.
[39] ISPRA Istituto Superiore per la Protezione e la Ricerca Ambientale, Serie Storiche Emissioni, (n.d.).
[40] Parrado C, Girard A, Simon F, Fuentealba E. 2050 LCOE (Levelized Cost of Energy) projection for a hybrid PV (photovoltaic)-CSP (concentrated solar power) plant in the Atacama Desert, Chile. Energy 2016;94:422–30. https://doi.org/10.1016/j.energy.2015.11.015.
[41] GME electricity market, (2023) https://www.mercatoelettrico.org/it/.
[42] W. Cole, A.W. Frazier, C. Augustine, Cost Projections for Utility-Scale Battery Storage: 2021 Update, United States, 2021. https://dx.doi.org/10.2172/1786976.
[43] Fares RL, Webber ME. What are the tradeoffs between battery energy storage cycle life and calendar life in the energy arbitrage application? J Energy Storage 2018; 16:37–45. https://doi.org/10.1016/j.est.2018.01.002.